The 2013 hot, dry summer in Western Europe

Article

Accepted Version

THE 2013 HOT, DRY SUMMER IN WESTERN EUROPE

BUWEN DONG, ROWAN SUTTON AND LEN SHAFFREY—National Centre for Atmospheric Science, Department of Meteorology, University of Reading, Reading, United Kingdom;

Summary

Anthropogenic forcing played a substantial part in Western Europe's hot, dry summer in 2013. North Atlantic sea surface temperatures were likely a factor in the large contrast with summer 2012.

Observations

Western Europe experienced sweltering high temperatures in summer 2013. On 22 July 2013, the United Kingdom recorded its hottest day since July 2006, with 33.5°C recorded at Heathrow and Northolt in west London (Met Office 2014). Averaged over Western Europe (Fig 1c), the seasonal mean (June–August) anomaly in surface air temperature (SAT) was 1.33°C above the mean over the period of 1964–93, which is 3.2 standard deviations of the interannual variability. [HadCRUT4 data (Morice et al. 2012) shows a similar warming of 1.28°C.] This magnitude of warming is slightly less but comparable with the previous hot summers in Western Europe, such as 2003 (e.g., Schaer et al. 2004) and 2010 (e.g., Barriopedro et al. 2011) for which summer mean SAT anomalies were 1.46°C and 1.86°C respectively, corresponding to 3.5 and 4.5 standard deviations.

The atmospheric circulation in summer 2013 was characterized by anomalously high sea level pressure (SLP) extending from the United Kingdom into northern Europe and anomalously low SLP over the Arctic (Fig. 1a). This pattern projects strongly onto the positive phase of the summer North Atlantic Oscillation (SNAO; Folland et al. 2009). The anomalous SNAO index of 2.7 hPa in 2013 was +1.0 standard deviation of the interannual variability, in stark contrast with the previous summer of 2012 for which the index was -2.7 standard deviations (Supplementary Fig. S1b). The circulation pattern in 2013 was associated with a northward shift of summer North Atlantic storm track (Fig. 1e and f). The climatology of cyclone track density (Dong et al. 2013a and Fig. 1e) shows a split into two preferred cyclone paths at the North Atlantic jet exit region (5°W–5°E): one passing near Iceland at

~71°N and into the Nordic Seas and the other passing across the British Isles at ~56°N and into Western Europe. In summer 2013, more storms than usual passed over Iceland and fewer over the United Kingdom and into Western Europe (Fig. 1f). This led to dry conditions in the United Kingdom and most of Western Europe. The area-averaged precipitation anomaly was –0.35 mm day^{-1}, which is –2.2 standard deviations of the interannual variability (Supplementary Fig. S1c). The low rainfall was also in stark contrast to the summer of 2012, which was a record wet summer in the United Kingdom and was last in a series of wet UK summers since 2007, each of which was associated with a negative SNAO index (Allan and Folland 2012; Dong et al. 2013b). [Note that the inhomogeneity of the data in E-OBS precipitation is a potential source of bias (Zolina et al. 2014), but negative precipitation anomalies in Western Europe are consistent with the northward shifted storm track.]

Global SST anomalies for summer 2013 are illustrated in Fig. 1d. Warm SSTs (relative to 1964–93) were present in many regions, with a prominent warm anomaly (> 1.0°C) along the Gulf Stream extension in the North Atlantic. Associated with this feature were an enhanced meridional SST gradient to the north and a reduced gradient to the south (Supplementary Fig. S2c). These anomalous SST gradients may have played a role in the observed northward shift of the North Atlantic storm track (e.g., Sampe et al. 2010; Ogawa et al. 2012) and influenced the related anomalies in the SNAO and Western European climate (Folland et al. 2009; Sutton and Dong 2012; Dong et al. 2013a). Warm anomalies were also observed in the Arctic, consistent with the continuing low sea ice extent (SIE); these SIE anomalies might also have had an influence on the atmospheric circulation (Balmaseda et al. 2010; Petrie et al. 2014).

Relative to the climatological period of 1964–93, by 2012 there were significant increases in anthropogenic greenhouse gas (GHG) concentrations (e.g., WMO 2013) and significant changes in anthropogenic aerosols. European and North American sulphur dioxide

emissions had declined while Asian emissions had increased (e.g., Lamarque et al. 2010). In this study, we investigate the roles of changes in SST, SIE, and radiative forcing in shaping the European summer of 2013, as well as possible reasons for the striking contrast between summer 2013 and summer 2012. Our focus is on seasonal mean conditions rather than on shorter-lived events that occurred within the season.

Climate model experiments

Climate model experiments have been carried out to identify the roles of changes in: (a) SST/SIE and (b) anthropogenic GHG and aerosol forcing in the European summer climate anomalies of 2013. In this study, we do not address the anthropogenic contribution to the SST/SIE changes, but rather consider these changes as an independent forcing factor. We use the atmosphere configuration of the Met Office Hadley Centre Global Environment Model version 3 (HadGEM3-A; Hewitt et al. 2011), with a resolution of 1.875° longitude by 1.25° latitude and 85 levels in the vertical. Dong et al. (2013b) used the same model to study the 2012 summer in Europe. A series of experiments was performed, the details of which are summarized in Table 1. We use the same control experiment (CONTROL) for the period 1964–93 as Dong et al. (2013b) and perform two other experiments: ALL2013 and SST2013. Both of these experiments use 2013 SST and SIE boundary conditions but they differ in the specification of anthropogenic GHG and aerosol forcing: ALL2013 uses anthropogenic forcing appropriate for 2013 while SST2013 uses the same anthropogenic forcing as for the CONTROL experiment, appropriate for 1964–93. The last 25 years of each experiment are used for analysis. The CONTROL experiment reproduces realistic climatological SLP and precipitation patterns for summer (Supplemental Fig. S10.2 of Dong et al. 2013b).

The model simulates a significant warming over Europe in summer 2013 in response to changes in SST, SIE, and anthropogenic forcing (i.e., ALL2013-CONTROL, Fig. 2a) with an area averaged SAT change of 1.11°C over Western Europe. The observed anomaly of

1.33°C is within the ±1 standard deviation range of the interannual variability of the model response (Supplementary Fig. S1a). Changes in SST and SIE explain 63% (±26%) of the area-averaged Western European warming response in HadGEM3 (Fig. 2d), with the remaining 37% (± 29%) explained by the direct impact (without forcing-induced SST and sea ice feedbacks) of changes in radiative forcings from GHG and aerosols (Fig. 2g and Supplementary Fig. S1a).

The atmospheric circulation anomalies simulated by the model (Fig. 2b) show notable similarities to the observed pattern over the North Atlantic and Europe (Fig. 1a), including low SLP anomalies over Greenland and an anomalous anticyclone over the United Kingdom. The wave train pattern of SLP anomalies suggests that changes in convection over the Caribbean Sea might be an important factor (e.g., Douville et al. 2011). However, in the model simulation the anomalous anticyclone does not extend as far eastward into central Europe as in the observations. The circulation anomalies correspond to a positive anomaly (mean = 1.2 hPa, which is only 0.5 standard deviations) in the SNAO index relative to the CONTROL, which is smaller than the observed anomaly (2.7 hPa; Supplementary Fig. S1b). The pattern of simulated Western European precipitation anomalies (Fig. 2c) is consistent with the positive phase of the SNAO and is similar to the observations, with anomalously low rainfall over most of Western Europe (Fig. 1b). As for the circulation anomaly, the magnitude of the mean precipitation anomaly is smaller than observed (Supplementary Fig S1c), although there is substantial interannual variability in the model results.

The additional SST2013 experiment suggests that *both* SST/SIE changes and the direct impact of changes in anthropogenic radiative forcing contributed to the anomalous circulation (Figs. 2e and h, Fig. S1b) and reduced rainfall over Western Europe in summer 2013 (Figs. 2f and i; Supplementary Fig. S1c). The SST change has the most impact on the low SLP anomalies simulated over Greenland, but GHG and aerosol forcing causes a

substantial anticyclonic anomaly over, and north of, the United Kingdom. This anticyclonic circulation anomaly is similar to the summer mean circulation response to an increase in GHG forcing (Blade et al. 2012) and is presumably due to an increase in the frequency of the positive SNAO-like circulation regimes over the Atlantic sector (Boe et al. 2009).

Changes in GHG and aerosol forcing are unlikely to be a major factor in explaining the striking contrast in circulation and precipitation between the European summers of 2012 and 2013 (Supplementary Fig. S2a), as the changes in these forcings between these two years were small. However, the model experiments suggest that changes in SST and SIE in the North Atlantic were a significant factor (Supplementary Fig. S2e). In particular, the anomalous meridional SST gradient to the north of the Gulf Stream in 2013, relative to 2012 (Supplementary Fig. S2c), may have favored a positive phase of the SNAO and a northward shift of North Atlantic summer storm track (e.g., Folland et al. 2009; Dong et al. 2013a), as was observed (Supplementary Figs. S2d and f). The model experiments show some evidence of capturing this shift, although the mean signal (Supplementary Fig. S2e) is again much weaker than was observed (Supplementary Fig. S2a).

The model results show an encouraging degree of consistency with observations, but it is difficult to assess precisely what level of consistency should be expected in view of the high level of internal variability and uncertainty about the true magnitude of forced signals in the real world. It is clear from Supplementary Fig. S1 that the signal-to-noise ratio for the changes in SAT is large, which permits more confident conclusions, whereas that for changes in circulation and precipitation is much lower (though it is interesting to note that the model suggests a stronger forced signal in Western European summer precipitation than in the SNAO). One limitation of the current experiments, which may well influence the signal-to-noise ratio, is the use of a prescribed SST boundary condition. Active ocean–atmosphere coupling may modify the response to forcings and is an important area of future work (Sutton

and Mathieu 2002; Dong et al. 2013a). Another extension not addressed here is the anthropogenic contribution to the SST/SIE changes.

Conclusions

The European summer of 2013 was marked by hot and dry conditions in Western Europe associated with a northward shifted Atlantic storm track and a positive phase of the SNAO. Model results suggest that, relative to a 1964–93 reference period, changes in SST/SIE explain 63% (±26%) of the area-averaged warming signal over Western Europe, with the remaining 37% (±29%) explained by the direct impact of changes in anthropogenic radiative forcings from GHG and aerosols. The results further suggest that the anomalous atmospheric circulation, and associated low rainfall, were also influenced both by changes in SST/SIE and by the direct impact of changes in radiative forcings; however, the magnitude of the forced signals in these variables is much less, relative to internal variability, than for surface air temperature. Further evidence suggests that changes in North Atlantic SST were likely an important factor in explaining the striking contrast between the European summers of 2013 and that of 2012. A major area for further work is to understand more completely the mechanisms that explain these influences.

REFERENCES:

Allan, R., and C. K. Folland, 2012: [Global climate] Atmospheric circulation: Mean sea level pressure. [In "State of the Climate 2011"]. *Bull. Amer. Meteor. Soc*., **93** (7), S35–S36.

Barriopedro, D., E. M. Fischer, J. Lutenbacher, R. M. Trigo, and R. Garcia-Herrera, 2011: The hot summer of 2010: redrawing the temperature record map of Europe. *Science*, **332**, 220–224.

Balmaseda, M. A., L. Ferranti, F. Molteni, and T. N. Palmer, 2010: Impact of 2007 and 2008 Arctic ice anomalies on the atmospheric circulation: Implications for long‐range predictions. *Quart. J. Roy. Meteor. Soc.*, **136**, 1655–1664.

Boé, J., L. Terray, C. Cassou and J. Najac, 2009: Uncertainties in European summer precipitation changes: role of large scale circulation. *Clim. Dyn.,* **33**, 265–276. doi:10. 1007/s00382-008-0474-7.

Bladé, I., B. Liebmann, D. Fortuny, and G. J. Oldenborgh, 2012: Observed and simulated impacts of the summer NAO in Europe: Implications for projected drying in the Mediterranean region, *Clim. Dyn*., **39**, 709–727, doi:10.1007/s00382-011-1195-x.

Dong, B., R. T. Sutton, T. Woollings, and K. Hodges, 2013a: Variability of the North Atlantic summer stormtrack: Mechanisms and impacts. *Environ. Res. Lett.*, **8**, 034037 doi:10.1088/1748-9326/8/3/034037

Dong, B.-W., R. T. Sutton, and T. Woollings, 2013b: The extreme European summer 2012 (in "Explaining Extreme Events of 2012 from a Climate Perspective"). *Bull. Amer. Meteor. Soc.,* **94** (9), S28–S32.

Douville, H., S. Bielli, C. Cassou, M. Dequé, N. M. J. Hall, S. Tyteca, and A. Voldoire, 2011: Tropical influence on boreal summer mid-latitude stationary waves. *Climate Dyn.*, **38**, 1783–1798.

Folland, C. K., J. Knight, H. W. Linderholm, D. Fereday, S. Ineson, and J. W. Hurrell, 2009: The summer North Atlantic oscillation: Past, present, and future. *J. Climate*, **22**, 1082–1103.

Haylock, M. R., N. Hofstra, A. M. G. Klein Tank, E. J. Klok, P. D. Jones, and M. New, 2008: A European daily high-resolution gridded dataset of surface temperature and precipitation for 1950–2006. *J. Geophys. Res.*, **113**, D20119, doi:10.1029/2008JD010201.

Hewitt, H. T., D. Copsey, I. D. Culverwell, C. M. Harris, R. S. R. Hill, A. B. Keen, A. J. McLaren, and E. C. Hunke, 2011: Design and implementation of the infrastructure of HadGEM3: The next-generation Met Office climate modelling system. *Geosci. Model Dev*., **4**, 223–253.

Hoskins, B. J., and K. I. Hodges, 2002: New perspectives on the Northern Hemisphere winter storm tracks. *J. Atmos. Sci.,* **59**, 1041–1061.

Kalnay, E., and Coauthors, 1996: The NCEP-NCAR 40-year reanalysis project. *Bull. Amer. Meteor. Soc.*, **77**, 437–471.

Lamarque, J.-F., and Coauthors, 2010: Historical (1850–2000) gridded anthropogenic and biomass burning emissions of reactive gases and aerosols: Methodology and application. *Atmos. Chem. Phys.*, **10**, 7017–7039, doi:10.5194/acp-10-7017-2010.

Met Office, cited 2014: Hot dry spell July 2013. [Available online at http://www.metoffice.gov.uk/climate/uk/interesting/2013-heatwave.]

Morice, C. P., J. J. Kennedy, N. A. Rayner, and P. D. Jones, 2012: Quantifying uncertainties in global and regional temperature change using an ensemble of observational estimates: The HadCRUT4 dataset, *J. Geophys. Res*., **117,** D08101, doi:10.1029/2011JD017187.

Ogawa, F., H. Nakamura, K. Nishii, T. Miyasaka, and A. Kuwano-Yoshida, 2012: Dependence of the climatological axial latitudes of the tropospheric westerlies and storm tracks on the latitude of an extratropical oceanic front. *Geophys. Res. Lett*., doi:10.1029/2011GL049922

Petrie, R., L. C. Shaffrey, and R. T. Sutton, 2014: The atmospheric response to Arctic sea ice decline. *Geophy. Res. Lett.,* (submitted).

Rayner, N. A., D. E. Parker, E. B. Horton, C. K. Folland, L. V. Alexander, D. P. Rowell, E. C. Kent, and A. Kaplan, 2003: Global analyses of sea surface temperature, sea ice, and night marine air temperature since the late nineteenth century. *J. Geophys. Res.,* **108** (D14), 4407, doi:10.1029/2002JD002670.

Sampe, T., H. Nakamura, A. Goto, and W. Ohfuchi, 2010: Significance of a midlatitude SST frontal zone in the formation of a storm track and an eddy-driven westerly jet. *J. Climate*, **23**, 1793–1814.

Schaer, C., P. L. Vidale, D. Luethi, C. Frei, C. Haeberli, M. A. Liniger and C. Appenzeller, 2004: The role of increasing temperature variability in European summer heatwaves. *Nature,* **427,** 332–336.

Sutton, R. T., and B.-W. Dong, 2012: Atlantic Ocean influence on a shift in European climate in the 1990s. *Nature Geosci.*, **5**, 788–792, doi:10.1038/ngeo1595.

Sutton, R. T., and P.P. Mathieu, 2002: Response of the atmosphere–ocean mixed-layer system to anomalous ocean heat-flux convergence. *Quart. J. Roy. Meteor. Soc.*, **128**, 1259–1275

WMO, 2013: The state of greenhouse gases in the atmosphere based on global observations through 2012. *WMO Greenhouse Gas Bulletin*, No. 9, 4 pp.

221 Zolina, O., and Coauthors, 2014: New view on precipitation variability and extremes in
222 Central Europe from a German high resolution daily precipitation dataset: Results
223 from STAMMEX project *Bull. Am. Meteorol. Soc.* at press (doi:10.1175/BAMS-D-
224 12-00134.1)

225

226 **Table 1.** Summary of numerical experiments.

Experiments	Boundary conditions	Length of run
CONTROL	Forced with monthly mean climatological sea surface temperature (SST) and sea ice extent (SIE) averaged over the period of 1964 to 1993 using HadISST data (Rayner et al. 2003) and with anthropogenic greenhouse gases (GHG) concentrations averaged over the same period and anthropogenic aerosols emissions averaged over the period of 1970 to 1993.	32 years
ALL2013	Forced with monthly mean SST and SIE from December 2012 to November 2013 using HadISST data, with anthropogenic GHG concentration in 2012 (WMO 2013) and anthropogenic aerosol emissions for 2010 (Lamarque et al. 2010), which is the most recent year for which emissions data were available.	27 years
SST2013	As ALL2013, but with anthropogenic GHG concentrations and anthropogenic aerosol emissions the same as in CONTROL.	27 years

227

228

Figure legends

FIGURE. 1. Anomalies for JJA 2013 from the climatological period 1964-1993 for (a) SLP (hPa) and (c) SAT (^{o}C) from NCEP reanalysis (Kalnay et al. 1996), (b) percentage precipitation change (%) from the daily gridded E-OBS precipitation (version 9.0) over Europe (Haylock et al. 2008) and (d) SSTs (^{o}C) from HadISST (Rayner et al. 2003). (e) and (h) for the climatological period and 2013 cyclone track density as in Hoskins and Hodges (2002) based on NCEP reanalysis. Track density is in unit of numbers per month per unit area, where the unit area is equivalent to a 5^{o} spherical cap (about 10^{6} km^{2}). Note that this climatological period is dominated by cold AMO conditions and is the period used for the climatological model simulations. Thick lines in (a) and (c) highlight regions where the differences are statistically significant at the 90% confidence level using a two-tailed Student t-test.

FIGURE. 2. SAT (^{o}C) (left column), SLP (hPa) (middle column) and precipitation changes (right column) (%) in the model simulations forced by different configurations of forcings in 2013 relative to the control simulation. (a), (b) and (c) forced by changes in SST and SIE, GHG concentrations, and aerosols emissions (ALL2013-CONTROL). (d), (e) and (f) forced by changes in SST and SIE (SST2013-CONTROL). (g), h) and (i) forced by changes in GHG and aerosols emissions (ALL2013-SST2013). Only changes that are statistically significant at the 90% confidence level using a two-tailed Student t-test are plotted in (a), (d) and (g) while thick lines in other panels highlight regions where the differences are statistically significant at the 90% confidence level.

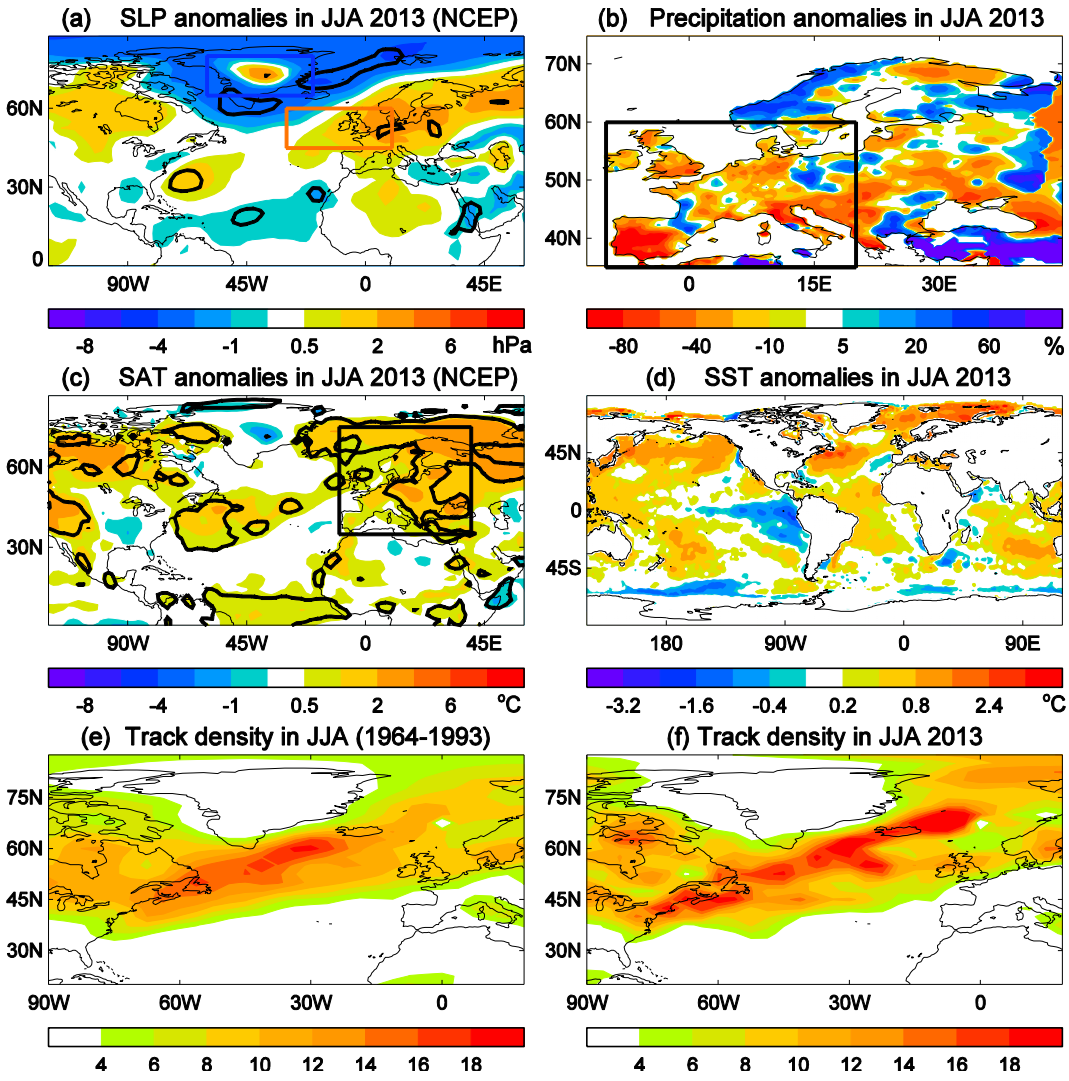

253

254 **FIGURE. 1.** Anomalies for JJA 2013 from the climatological period 1964-1993 for (a) SLP
255 (hPa) and (c) SAT (^{o}C) from NCEP reanalysis (Kalnay et al. 1996), (b) percentage
256 precipitation change (%) from the daily gridded E-OBS precipitation (version 9.0) over
257 Europe (Haylock et al. 2008) and (d) SSTs (^{o}C) from HadISST (Rayner et al. 2003). (e) and
258 (h) for the climatological period and 2013 cyclone track density as in Hoskins and Hodges
259 (2002) based on NCEP reanalysis. Track density is in unit of numbers per month per unit
260 area, where the unit area is equivalent to a 5^{o} spherical cap (about 10^{6} km^{2}). Note that this
261 climatological period is dominated by cold AMO conditions and is the period used for the
262 climatological model simulations. Thick lines in (a) and (c) highlight regions where the
263 differences are statistically significant at the 90% confidence level using a two-tailed Student
264 t-test.

265

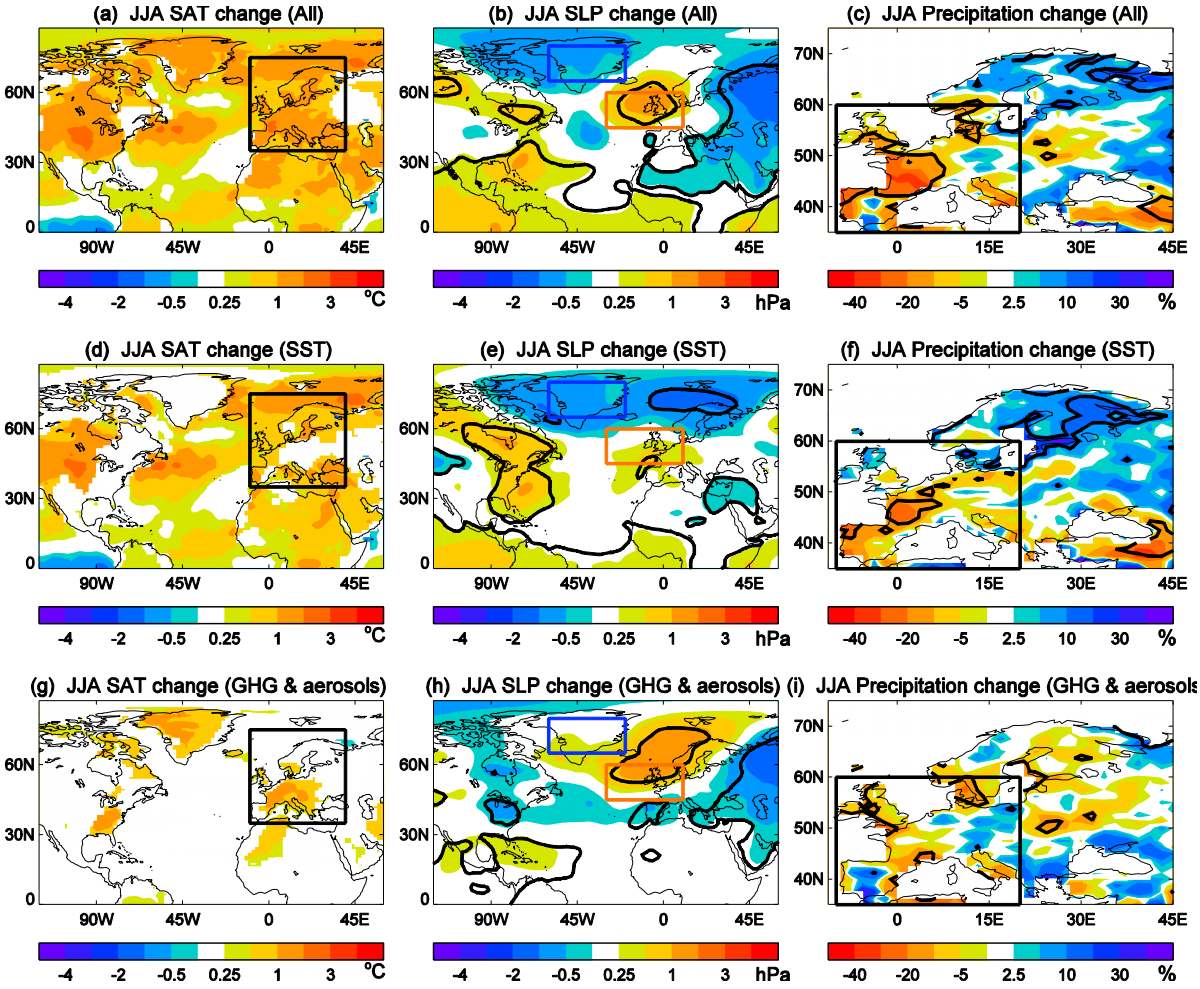

FIGURE. 2. SAT (°C) (left column), SLP (hPa) (middle column) and precipitation changes (right column) (%) in the model simulations forced by different configurations of forcings in 2013 relative to the control simulation. (a), (b) and (c) forced by changes in SST and SIE, GHG concentrations, and aerosols emissions (ALL2013-CONTROL). (d), (e) and (f) forced by changes in SST and SIE (SST2013-CONTROL). (g), h) and (i) forced by changes in GHG and aerosols emissions (ALL2013-SST2013). Only changes that are statistically significant at the 90% confidence level using a two-tailed Student t-test are plotted in (a), (d) and (g) while thick lines in other panels highlight regions where the differences are statistically significant at the 90% confidence level.

SUPPLEMENTAL MATERIALS: THE 2013 HOT, DRY SUMMER IN WESTERN EUROPE

BUWEN DONG, ROWAN SUTTON AND LEN SHAFFREY

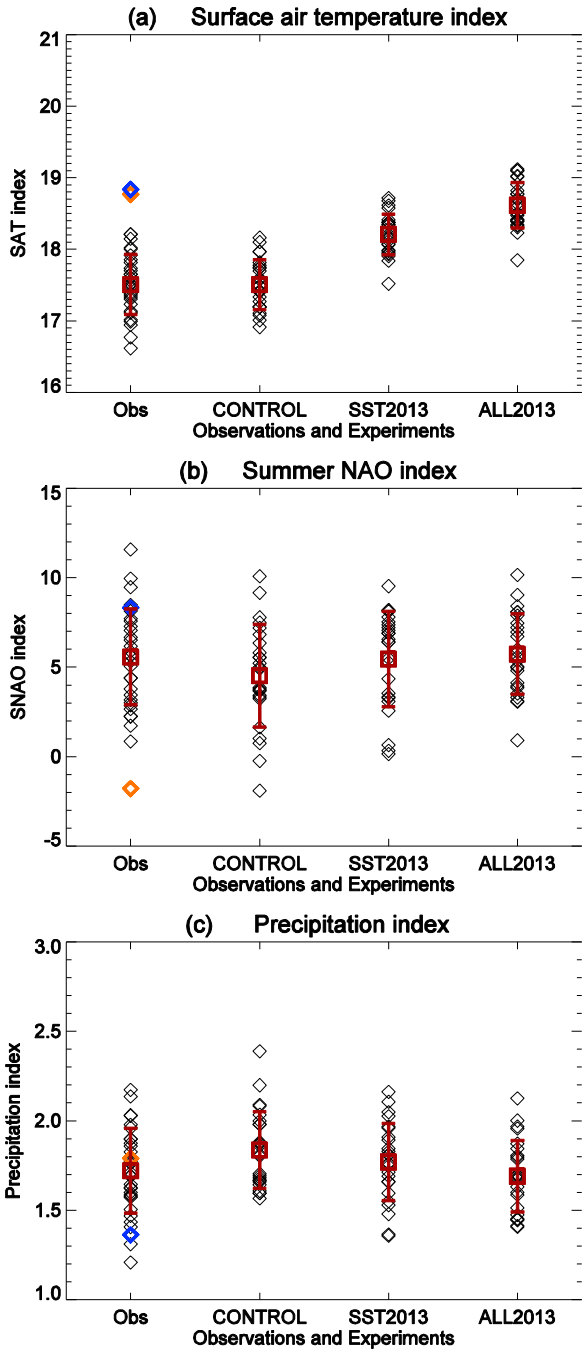

Figure S1: (a) SAT (^{o}C), (b) summer NAO (hPa), and (c) precipitation (mm day^{-1}) indices for observations and model experiments. SAT index is area averaged SAT over region (35^{o}N-75^{o}N, 10^{o}W-40^{o}E, land only) (black box in Fig.1c). The SNAO index is defined as the difference of the area mean SLP between two regions around the British Isles (45^{o}-60^{o}N, 30^{o}W-10^{o}E) and over Greenland (65^{o}N-80^{o}N, 60^{o}W-20^{o}W) (red and blue boxes in Fig. 1a). Precipitation index is area averaged precipitation over region (35^{o}N-60^{o}N, 10^{o}W-20^{o}E, land only) (black box in Fig.1b). All black diamonds in observations are for years from 1964 to 1993 with red diamonds for 2012 and blue diamonds for 2013. Red squares and lines are the mean and mean ± sigma ranges where sigma is the corresponding standard deviation.

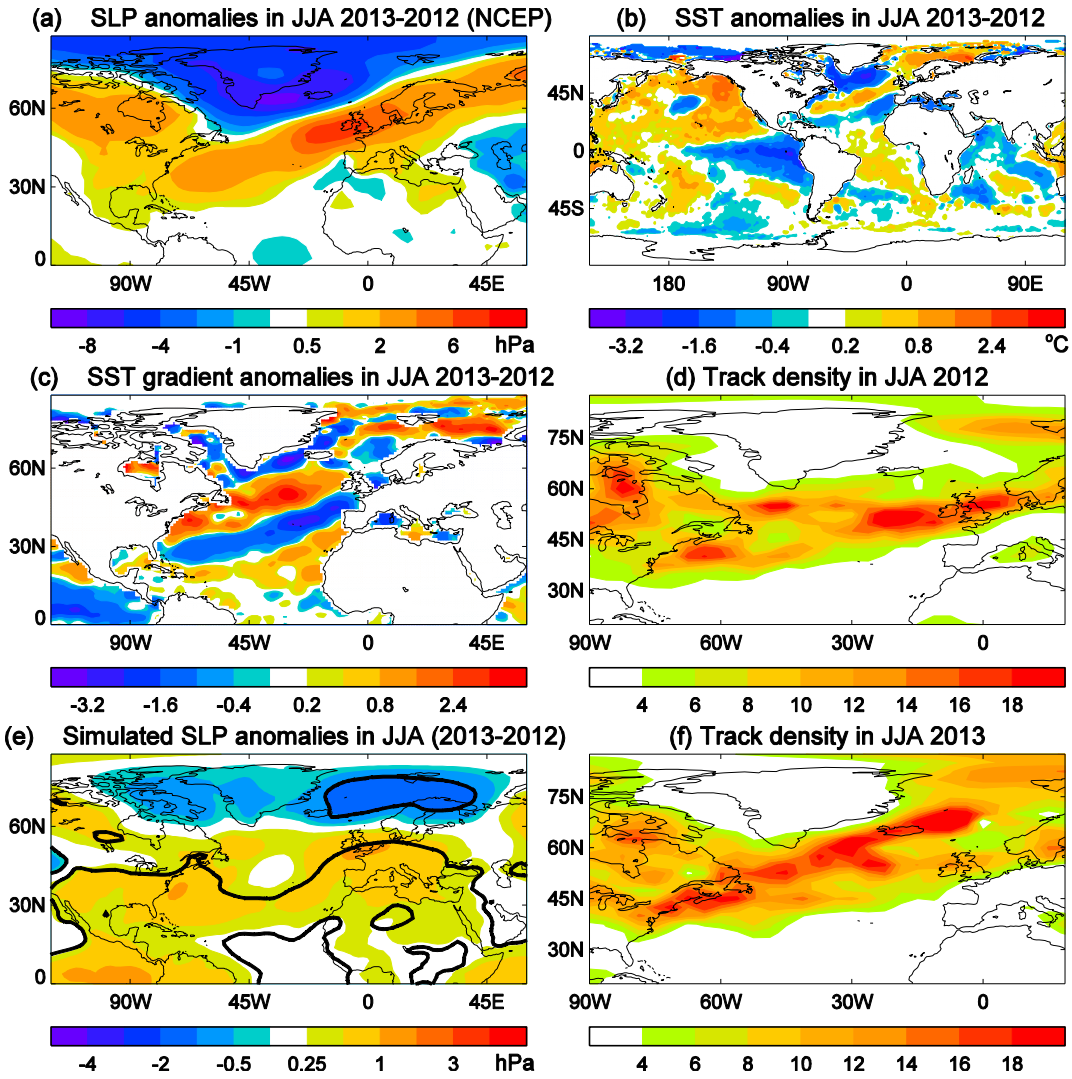

Figure S2. Anomalies in JJA between 2013 and 2012. (a) SLP (hPa), (b) SST (^{o}C), and (c) SST gradient (^{o}C per 1000 km) in observations. (e) Simulated SLP difference between 2013 and 2012 from the changes in SST and SIE. The experiment of 2012 was documented in Dong et al. (2013b). (d) and (f) are 2012 and 2013 cyclone track density. Track density is in unit of numbers per month per unit area, where the unit area is equivalent to a 5^{o} spherical cap (about 10^{6} km^{2}). Note that this climatological period is dominated by cold AMO conditions and is the period used for the climatological model simulations. Thick lines in (e) highlight regions where the differences are statistically significant at the 90% confidence level using a two-tailed Student t-test.